Preliminary Study on the Onset of Necking Detection Using DIT in Tensile Tests

D. Palomo[*,a], A.J. Martinez-Donaire[*,b], J.A. Lopez-Fernandez[c], M. Borrego[d] and   C. Vallellano[e]

Department of Mechanical and Manufacturing Engineering, University of Seville, Spain

[a]dpalomo1@us.es, [b]ajmd@us.es, [c]jlopez85@us.es, [d]mborrego@us.es, [e]carpofor@us.es

Keywords: Sheet metal forming, Local necking, Digital infrared thermography, Tensile test.

Abstract. The experimental detection of localized necking is an important issue in sheet metal forming. Today, the most common and extended techniques are strain-based methods using digital image correlation (DIC). The present work discuses a thermal methodology to detect the onset of necking in metals based on the analysis of the temperature gradient using digital infrared thermography (DIT). A series of tensile tests of H240LA-O3 high-strength steel of 1.2mm thickness is analysed using DIC and DIT techniques. It is proposed that necking initiates when the temperature difference ΔT at a reference distance from the necking point reaches a critical value, which allows identifying the necking time and estimating the limit strains from the visible images using circle grid analysis.

Introduction

Thermal effects of heat generation during the plastic deformation of metals have been analysed for decades. One of the most relevant works was presented by Taylor and Quinney [1], who studied the relation between thermal and mechanical material properties, quantifying the fraction of plastic work converted to heat. This is defined by the very well-known Taylor-Quinney coefficient, which is dependent on the material properties and the deformation process conditions, mainly the strain rate [2,3].

The experimental detection of localized necking in sheet metal forming using strain-based methods is the most common and extended technique nowadays [4]. Apart from standardized approaches focused on measuring the strain in the postmortem specimen, more reliable accurate methods using digital image correlation (DIC) require still expensive commercial devices and software. A less explored alternative is to analyse the temperature field created during plastic deformation by means of digital infrared thermography (DIT).

Chrysochoos and Louche [5] analysed the stored energy during the necking process using coupled DIC and DIT systems. Maj et al. [6] examined the onset of necking in tensile tests of austenitic stainless steel 304L and aluminium alloy (PA6) at displacement rates of 100 mm/min, 1000 mm/min and 2000 mm/min. They established that necking appeared when the variation on temperature or strain between two reference points reached a critical value, that is, 1ºC and 0.01, respectively. Recently, Soares et al. [7] have studied the thermomechanical response of AISI301 in tensile tests. They observed that temperature increased homogeneously during uniform deformation for strain rates from 0.01 to 900 s^{-1} and increased markedly with the onset of necking in the region of localized strain, pointing out that both the localized increase of strain and temperature during necking are synchronized in position and time.

This work presents a preliminary analysis to establish an experimental methodology to detect the onset of necking in metals based on the analysis of the temperature gradient using DIT, as an alternative to the ones using strain gradient analysis using DIC. The assumption of Maj et al. [6] based on the existence of a critical temperature increment at initiation of the neck is explored to detect the necking time. The necking strains are measured using circle grid analysis and compared with the ones obtained using the time dependent method proposed by Martinez-Donaire et al. [4]. The material tested was H240LA-O3 high-strength steel in 1.2mm thickness sheets.

Table 1. Chemical composition of H240LA-O3 steel.

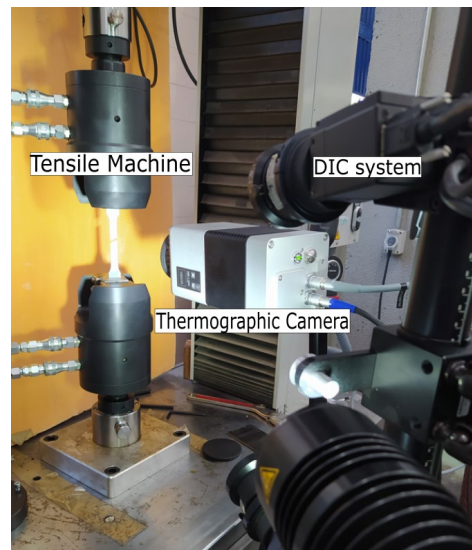| C (%)	Mn (%)	Si (%)	P (%)	S (%)	Al (%)	Ni (%)	Ti (%)
0,0746	0,3071	0,0100	0,0093	0,0142	0,0346	0,0137	0,0021

Figure 1. Experimental setup of tensile tests including the ARAMIS CCD cameras and the infrared camera in front of the specimen (visible camera is not shown).

Experimental Procedure

The experiments were performed on sheet of H240LA-O3 high-strength low alloy steel of 1.2 mm thickness with the chemical composition shown in Table 1.

A series of tensile tests were carried out on an Instrom 1196 testing machine according to the ASTM E8 standard. The gage length and width of the specimen were 60 mm and 12.5mm, respectively. Two displacement rates, 80 mm/min and 100 mm/min, were analyzed. The displacement and temperature fields during the tensile test were measured using synchronized DIC and DIT systems. Figure 1 shows the experimental setup.

The commercial ARAMIS® system was used to measure the strains. The front face of the specimen was painted with a stochastic black dot pattern on a white background that was easily recognizable by the ARAMIS® software. The spatial evolution of the dot pattern was recorded during the test using two 5MPx digital CCD cameras and latter converted into strains. Thermal evolution was measured using an Infratec VarioCAM HD head 600 camera operated by IRBIS3® software. This allowed capturing the thermal information of an area of 640x480 pixels.

The rear face of the sample was electrochemically marked with a regular circle pattern of 0.75 mm in diameter and a distance between centers of 1.5 mm. The evolution of this face was recorded via a regular visible camera (Source 5MPx visible camera) with the aim of measuring the strains via circle grid analysis without the need for the DIC system.

The three systems (ARAMIS® cameras, infrared camera and visible camera) were synchronized to take images at the same time and frequency. The ARAMIS® software acted as a master system, triggering the image acquisition process. At the end of the test, a map of the strains and temperature evolution with time is obtained and used to analyze the appearance of the local necking.
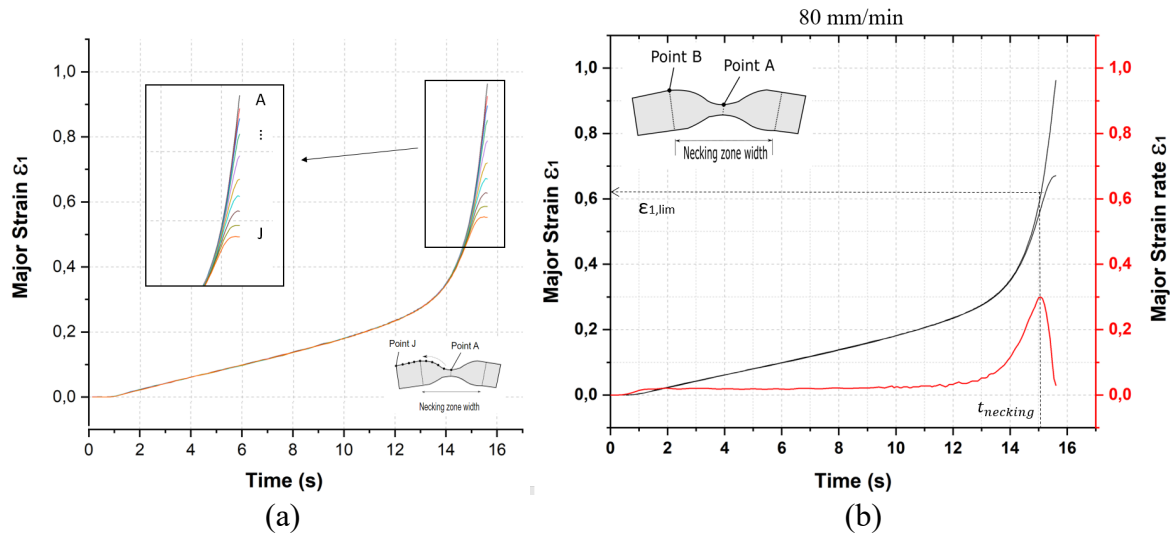
Figure 2. Experimental time evolution of ε_1 of a series of points along a cross section perpendicular to the crack (a) and identification of the time of necking and the major limit strain at necking (b) for the tensile test T1 at 80mm/min.

Table 2. Major limit strain at necking and time of necking for tensile tests at 80 and 100 mm/min.

	displacement rate			
	80 mm/min		100 mm/min	
	Test 1	**Test 2**	**Test 1**	**Test 2**
$\varepsilon_{1,lim}$	0.63	0.61	0.58	0.57
$t_{necking}$ (s)	15.13	14.42	11.00	12.12

Strain at necking

Before analysing the temperature evolution at necking it is crucial to precisely know the moment of appearance of the neck and the major strain at that instant. To this end, the time-dependent methodology proposed by Martinez-Donaire et al. [4] based on the experimental evidence of the necking initiation and development is used.

Briefly, the method makes use on the temporal analysis of the major strain distribution and its first time derivative ($\dot{\varepsilon}_1$, "major strain rate") of two representative points in the necking zone just before the crack appears. Figure 2(a) depicts the time evolution of ε_1 of a series of points along a cross section perpendicular to the crack for a tensile test at 80mm/min (T1 in Table 2). The evolution of the two representative points is shown in Figure2(b). The first representative point is the necking initiation point, identified as the point exhibiting the highest strain evolution (point A). The second one is a point at the boundary of the necking region, defined as first point in the necking zone (on both sides of the crack) that stops straining, reaching therefore zero major strain rate at that instant (point B). The onset necking is established at the instant ($t_{necking}$) that the strain rate at point B reaches a local maximum (see red line in Fig, 2(b)). The major limit strain at necking ($\varepsilon_{1,lim}$) is defined as the strain at point A at that time (see Fig. 2(b)).

Table 2 shows the major limit strain at necking and time of necking for at 80 and 100 mm/min. These tests are divided in two groups: the T1 tests used to propose the thermal method of necking detection and the T2 tests used to validated the proposed method.
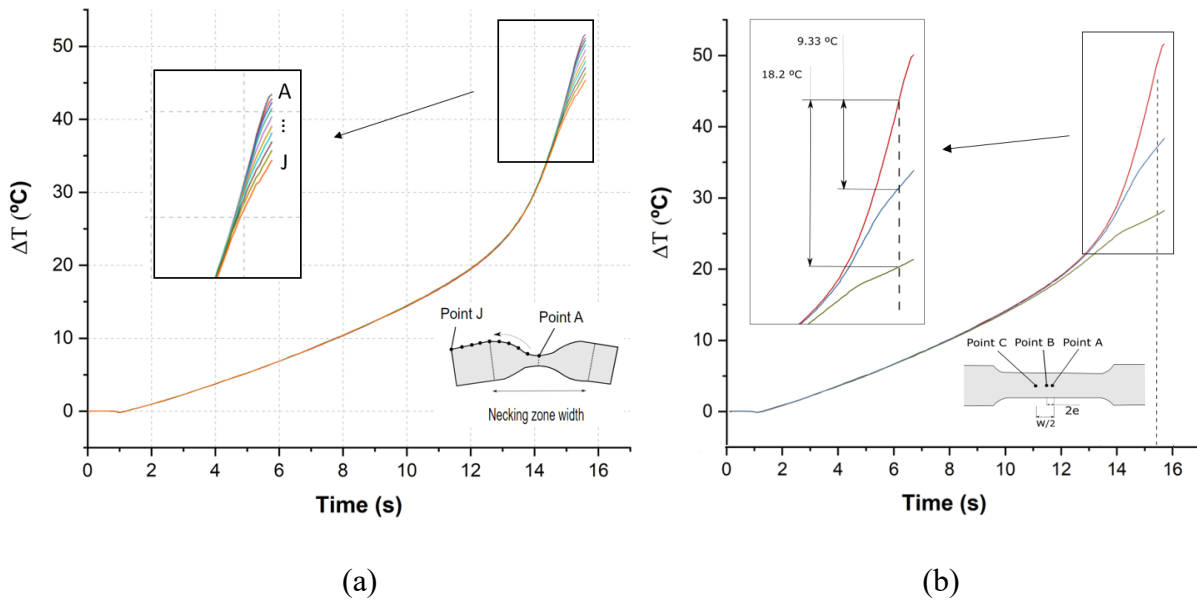
(a)　　　　　　　　　　　　　　　　　(b)

Figure 3. Experimental time evolution of ΔT of a series of points along a cross section perpendicular to the crack (a) and temperature difference at $2e$ and $w/2$ distances at the time of necking (b) for the tensile test T1 at 80mm/min.

Table 3. Temperature difference ΔT for distances from the necking initiation equal to $e/2$, e, $2e$, $w/2$, and w in the T1 tests for 80 and 100 mm/min.

	Test T1 - 80 mm/min		Test T1 -100 mm/min			
	Left (°C)	Right (°C)	Left (°C)	Right (°C)	Mean value (°C)	Error (%)
$\Delta T_{e/2}$	1.9	1.8	1.9	1.8	1.85	3
ΔT_e	5.0	4.5	5.1	4.6	4.8	7
ΔT_{2e}	9.3	9.4	9.3	9.2	9.3	1
$\Delta T_{w/2}$	18.2	18.7	18.9	19.0	18.7	2
ΔT_w	25.6	26.5	25.2	27.1	26.1	3

Temperature gradient at necking. Thermal method

In this section, the temperature gradient around the fracture zone of the tensile specimens is analyzed to establish an objective criterion to detect the onset of necking.

Figure 3 (a) shows the time evolution of the temperature of a series of points along a cross section perpendicular to the crack for a tensile T1 test at 80mm/min. As can be seen, the temperature increases uniformly with time at the beginning of the test, during the uniform plastic deformation of the specimen. Temperature gradients are not observed at this stage. The temperature gradient is observed once the deformation starts localizing to form the neck, becoming more evident at the end of the test. The main difference in the temperature evolution of Fig. 3(a) from the strain evolution shown in Fig. 2(a) is that the temperature always increases around the necking region. As a result, the boundary of the necking zone is not as obvious as in the strain analysis.

According to Maj et al. [6], it can be assumed that the initiation of necking produces a characteristic local heat gradient such that it can be detected by establishing a critical temperature difference (ΔT) between the necking initiation point (A in Fig. 3(a)) and a reference point outside the neck. This critical temperature increment can be considered a material constant.
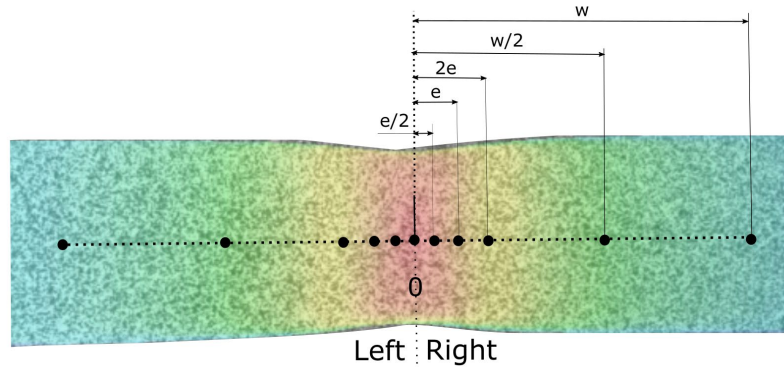
Fig 4. Distribution of distances ($e/2, e, 2e, w/2$, and w) in the necking area.

To explore the above assumption, the temperature difference ΔT between different points are obtained at the necking time given in the previous strain analysis. Figure 3(b) depicts the temperature evolution for the T1 test at 80 mm/min. The ΔT at the necking time for $2e$ and $w/2$ at the left-hand side of the neck is shown, having a value of 9.3ºC and 18.2 ºC, respectively. e and w are the sheet thickness and the specimen width, respectively. The ΔT for distances from the necking initiation equal to $e/2, e, 2e, w/2$, and w are also analysed. Figure 4 shows a comparative distribution in the necking area of these distances on both sides of the neck.

Table 3 shows ΔT at the above distances at both side of the neck, along with the mean value, for T1 tests at 80 and 100mm/min displacement rate. The maximum error is also depicted. As can be seen, the scatter of ΔT at $2e$ is very narrow, given a maximum error around 1%. As a result, it can be assumed that the necking appears in the tensile test when the temperature difference ΔT for a distance of $2e$ from the necking point reaches a critical value of 9.3ºC for the H240LA-O3 steel.

It should be noted that the extension of this approach to other materials will require an initial calibration, similar to the one described above, for setting the critical temperature difference (ΔT) that triggers failure by necking. This value will mainly depend on the thermal properties of the tested material.

Table 4. Time of necking and limit major strain using the thermal methodology for T2 tests at 80 and 100 mm/min.

Step	Test T2 - 80 mm/min				Test T2 -100 mm/min			
	$\Delta T_{2e\ LEFT}$ (ºC)	$\Delta T_{2e\ RIGHT}$ (ºC)	$t_{necking}$ (s)	$\varepsilon_{1,lim}$ (average)	$\Delta T_{2e\ LEFT}$ (ºC)	$\Delta T_{2e\ RIGHT}$ (ºC)	$t_{necking}$ (s)	$\varepsilon_{1,lim}$ (average)
n	9.2	9.7	14.35	0.58	9.0	9.0	12.12	0.53
n+1	9.9	10.7	14.42	0.61	10.0	10.3	12.19	0.57
				0.59				**0.55**

Thermal method validation

In the following, the T2 tensile tests will be used to validate the thermal criterion above. The thermal method is deployed in three steps:

1. The necking point is identified as the point where the crack begins in the last frame recorded before the fracture.
2. From the evolution of the temperature field, the necking time is determined as the instant at which the temperature difference ΔT at a distance of $2e$ from the necking point reaches a value of 9.3ºC (for H240LA-O3 steel sheets).
3. At the time of necking, the image of the visual camera is identified. The limit strains (major and minor) are estimated by measuring the major and minor diameter of the ellipses at the necking zone.
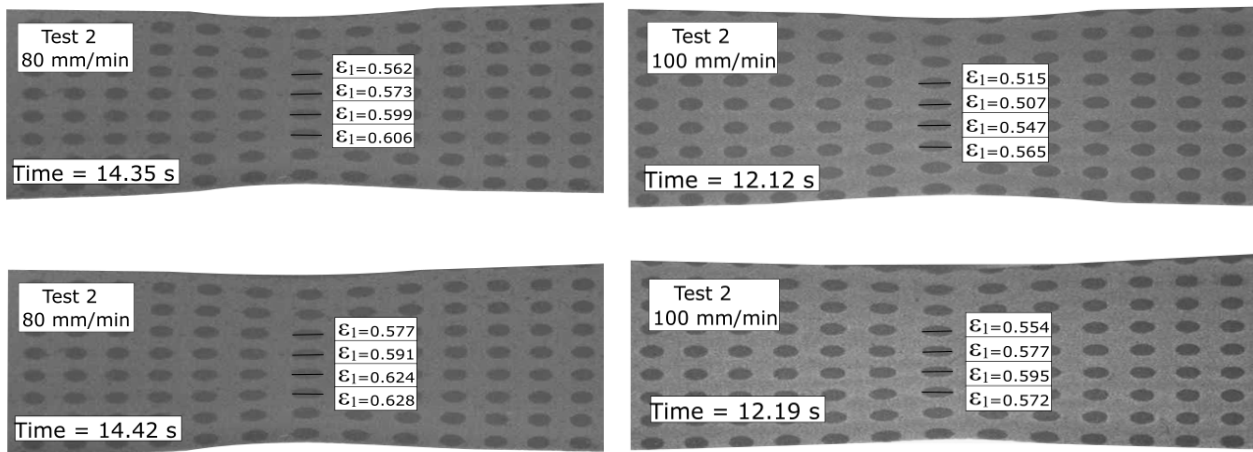
Figure 5. Major limit strain measurements in the visible images for T2 tests at 80mm/min (left) and 100 mm/min (right).

Table 4 shows the results of applying the thermal method to T2. Due to the impossibility of having data right at ΔT_{2e} of 9.3ºC, the time of necking and the limit strain are obtained as average of the values at the steps just above and below the threshold value. Figure 5 shows the strain measurements carried out in the visible images. As can be seen, the average major limit strain estimated is 0.59 and 0.55 for 80 and 100 mm/min displacement rate, respectively. These values agree well with the values obtained using the time-dependent method (see Table 2), although slightly underestimating them. The error remains below -3.5% in both tests.

Conclusions

A thermal methodology to detect the onset of necking in metals based on the analysis of the temperature gradient using DIT is discussed. A series of tensile tests over H240LA-O3 high strength steel of 1.2mm thickness is analysed using DIC and DIT techniques. It is possible to establish that necking initiates when the temperature difference ΔT at twice the specimen thickness from the necking point reaches a critical value. For the H240LA-O3 this value is 9.3ºC. This allows identifying the necking time and estimating the limit strains from the visible images at that instant using circle grid analysis. This thermal methodology is a cheaper and simpler alternative than the current methodologies based on strain analysis using DIC.

Acknowledgements

References

[1] G. Taylor, H. Quinney. The latent energy remaining in a metal after cold working. Proc R Soc Lond 143 (1934) 307–326.

[2] M. San Juan, O. Martín, F.J. Santos, P. De Tiedra, F. Daroca, R. López. Application of thermography to analyse the influence of the deformation rate in the forming process. Procedia engineering 63 (2013) 821-828.

[3] B.A. Behrens, A. Chugreev, F. Bohne, R. Lorenz. Approach for modelling the Taylor-Quinney coefficient of high strength steels. Procedia Manufacturing 29 (2019) 464-471.

[4] A.J. Martínez-Donaire, F.J. García-Lomas, C. Vallellano, New approaches to detect the onset of localized necking in sheets under through-thickness strain gradients, Materials & Design 57 (2014) 135-145.

[5] A. Chrysochoos, H. Louche. An infrared image processing to analyse the calorific effects accompanying strain localisation. International Journal of Engineering Science 38 (2000) 1759-1788.

[6] M. Maj, W. Oliferuk. Analysis of plastic strain localization on the basis of strain and temperature fields. Archives of metallurgy and materials 57 (2012) 1111-1116.

[7] G.C. Soares, N.I. Vázquez Fernández, M. Hokka. Thermomechanical Behaviour of Steels in Tension Studied with Synchronyzed Full-Field deformation and Temperature Measurements. Experimental Techniques 45 (2021) 627-643.